

Magnesium abundances in mildly metal-poor stars from different indicators

C. Abia¹, L. Mashonkina²

¹ *Departamento de Física Teórica y del Cosmos. Universidad de Granada, 18071 Granada, Spain*

² *Department of Astronomy, Kazan State University, Kremlevskaya 18, 420008 Kazan 8, Russia*

ABSTRACT

We present magnesium abundances derived from high resolution spectra using several Mg I and two high excitation Mg II lines for 19 metal-poor stars with $[\text{Fe}/\text{H}]$ values between -1.1 and $+0.2$. The main goal is to search for systematic differences in the derived abundances between the two ionisation state lines. Our analysis shows that the one-dimensional LTE and N-LTE study finds a very good agreement between these features. The $[\text{Mg}/\text{Fe}]$ vs. $[\text{Fe}/\text{H}]$ relationship derived, despite the small sample of stars, is also in agreement with the classical figure of increasing $[\text{Mg}/\text{Fe}]$ with decreasing metallicity. We find a significant scatter however, in the $[\text{Mg}/\text{Fe}]$ ratio at $[\text{Fe}/\text{H}] \sim -0.6$ which is currently explained as a consequence of the overlap at this metallicity of thick and thin disk stars, which were probably formed from material with different nucleosynthesis histories. We speculate on the possible consequences of the agreement found between Mg I and Mg II lines on the very well known oxygen problem in metal-poor stars. We also study the $[\text{O}/\text{Mg}]$ ratio in the sample stars using oxygen abundances from the literature and find that the current observations and nucleosynthetic predictions from type II supernovae disagree. We briefly discuss some alternatives to solve this discrepancy.

Key words: stars: abundances - stars: atmospheric parameters - Galaxy: chemical evolution

1 INTRODUCTION

It is currently assumed that the chemical composition of the atmospheres of unevolved (dwarf) stars reflects that of the material from which the stars are formed. Therefore, abundance studies in these stars covering a wide range of metallicities is probably the best tool to study the different scenarios proposed for the formation of the Galaxy, its star formation rate history and chemical evolution.

During the last decade there has been a considerable improvement in stellar abundance analyses. This fact, together with the more accurate derivation of the basic stellar parameters (effective temperature, gravity etc), mainly after the general use of the *Hipparcos Catalogue* data (ESA 1997), has considerably reduced the uncertainty in the derivation of stellar abundances; formal errors of a few hundredths of dex in the abundance ratios are now being obtained! (see e.g. Reddy et al. 2003). On the other hand, the classical LTE abundance analysis using 1D model atmospheres is being progressively replaced by full N-LTE abundance analysis, in some cases using also 3D hydrodynamical model atmospheres (Nordlund & Dravins 1990; Asplund et al. 1999;

Asplund & García-Pérez 2001). With such strong tools available, recent analyses of the abundance ratios ($[\text{X}/\text{Fe}]$) as a function of the stellar metallicity ($[\text{Fe}/\text{H}]$ ¹) are showing a new, detailed structure in the $[\text{X}/\text{Fe}]$ vs. $[\text{Fe}/\text{H}]$ trends (on occasions, unexpected) that were hidden in previous analyses, in part due to lower quality data and larger abundance errors (e.g. Gratton et al. 1996; Nissen & Schuster 1997; Fuhrmann 1998; Idiart & Thévenin 2000; Prochaska et al. 2000; Mashonkina & Gehren 2001; Gehren et al. 2004; Gratton et al. 2003a,b). These new studies clarify theories of the Galaxy's formation (see e.g. Weimberg et al. 2002; Samland & Gerhard 2003), in particular its star formation history, the timescales for the formation of the halo, thick and thin disks and, in some cases, could lead to a revision of the nucleosynthesis theory in stars, mainly in type II supernova explosions. For instance, concerning the well known overabundances of the named α -elements (O, Mg,

¹ The usual bracket notation is used throughout the paper for the abundance of an element X with respect to the hydrogen $[\text{X}/\text{H}] = \log \frac{(N_{\text{X}}/N_{\text{H}})_\star}{(N_{\text{X}}/N_{\text{H}})_\odot}$, where N represents number density.

Si, Ca etc) with respect to Fe in metal-poor stars, there are claims indicating that the level of this overabundance at a given metallicity is different depending on the stellar population studied: halo, thick-disk or thin-disk stars, but also for a particular α -element. This poses a difficult challenge to our current understanding of nucleosynthesis in stars. Furthermore, abundance studies in extreme metal-poor stars ($[\text{Fe}/\text{H}] < -2.5$) have revealed very peculiar abundance ratios. For instance, there are a significant number of stars with $[\text{C}, \text{N}, \text{Mg}, \text{Si}/\text{Fe}] > 1$, with a considerable degree of dispersion (Norris, Ryan & Beers 2001; Depagne et al. 2000; Truran et al. 2002; Aoki et al. 2002, among many others). This might well provide information about the level of mixing of the interstellar medium at early epochs as well as on nucleosynthesis processes in zero metallicity stars.

A common characteristic of many stellar abundance analyses is that they are usually based on the use of a small number of atomic lines for a specific element, in many cases also in the same ionisation state. Of course, for some elements there are very few spectral lines available in dwarf stars, in some cases just one (e.g. the Li I at 6708 Å) but in others, the use of several abundance indicators does not always lead to agreement between them. In fact, in this era of precision in abundance analyses, the longstanding problem of the $[\text{O}/\text{Fe}]$ vs. $[\text{Fe}/\text{H}]$ relationship in metal-poor stars still remains to be solved. The *oxygen problem* is that several potential indicators of the oxygen abundance (ultraviolet OH lines, the forbidden $[\text{OI}]$ 6300 Å and 6363 Å lines, the high excitation lines of 7770 Å O I triplet, and the near infrared vibration-rotation lines from the OH molecule's ground state), may give different results (see the recent discussions by Nissen et al. 2002, and Fulbright & Johnson 2003, for details). This fact provokes some doubts regarding our current understanding of line formation in the atmosphere of metal-poor stars and, in consequence, regarding the implications to be drawn from the abundance analyses for the important nucleosynthetic and galactic issues mentioned above.

In this paper, we address the difficulty using an example: magnesium. It is widely accepted that the $[\text{Mg}/\text{Fe}]$ ratio in metal-poor stars increases for decreasing metallicity, reaching a plateau-like value $\sim 0.3 - 0.4$ dex at $[\text{Fe}/\text{H}] \leq -1$. Magnesium is an α -element which is produced in the interior of massive stars during the hydrostatic burning phases of the stellar evolution. Nevertheless, recent studies have revealed that the $[\text{Mg}/\text{Fe}]$ ratio shows greater scattering at a given metallicity than other α -elements like, Si, Ca or Ti (we exclude here O); moreover, there is a sudden increase in the $[\text{Mg}/\text{Fe}]$ ratio at $[\text{Fe}/\text{H}] \sim -0.6$ and/or a clear distinction of the $[\text{Mg}/\text{Fe}]$ ratio depending on which population the star belongs to (see e.g. Prochaska et al. 2000; Qiu et al. 2003 and references therein).

Similarly to oxygen, there are several atomic and molecular Mg lines available to derive the abundance of this element in dwarfs, including two Mg II lines at 7787 and 7796 Å not commonly used in the literature and which have a similar excitation energy ($\chi = 9.99$ eV) to those of the O I triplet ($\chi = 9.14$ eV). From the point of view of classical 1D analysis, this implies that these Mg II lines should form at essentially (however, see below) the same depth in the atmosphere as the oxygen triplet lines. Furthermore, since neutral oxygen and single ionised magnesium are both ma-

jority species in metal-poor dwarf stars, they are expected to be affected in a similar way by stellar inhomogeneities (granulation, Asplund 2003). Furthermore, given the high excitation energy of these lines, they are expected to be as sensitive to the temperature structure of the atmosphere as the oxygen triplet. Departures from LTE in these Mg II lines are also expected, for the same reason. In brief, we wonder whether analysis of these Mg II would give abundances in agreement with those obtained with the more commonly used Mg I lines or, similarly to oxygen, there is also a *magnesium problem*.

The paper is organised as follows: Section 2 describes the observations and the sample of stars. Section 3 presents the abundance analysis of the selected Mg I and Mg II lines considering also the corrections for N-LTE effects. In Section 4 the results are compared with previous studies and finally our conclusions are summarised in Section 5.

2 OBSERVATIONS AND DATA REDUCTION

The magnesium and iron abundances were derived from spectra obtained with the SOFIN echelle spectrograph (Touminen et al. 1998) at the 2.5m NOT telescope in the Roque de los Muchachos Observatory on 9-11 January 2001. Using the first camera and the appropriate slit width (38 μm , corresponding to two pixels on the CCD), the resolving power achieved was $\sim 170000^2$. The spectral range 4850-10100 Å was observed simultaneously although with large gaps between the different spectral orders. Unfortunately, in the stars observed with this instrument, this limited the number of Mg I and iron lines available for the analysis. Therefore, comparison between Mg I and Mg II absolute abundances in the stars observed with SOFIN may lack some significant statistics: apart from the two Mg II lines, these spectra include only the Mg I line at 5711 Å. This was not the case, however, for the stars observed with the 2.2m telescope at Calar Alto Observatory on 18-20 July 2000 and 9-10 August 2003 using the echelle spectrograph FOCES (Pfeiffer et al. 1998). In this case the spectra covered the full range between 4400-9000 Å, at the cost of the lower resolving power (~ 40000) achieved. These spectra, hence, contain numerous Mg I and Fe II lines although, unfortunately, the Mg II 7877 Å line was placed near the border of the detector, where efficiency is not good. This meant that for some stars this line could not be used.

The spectra were reduced using IRAF following standard techniques for the extraction and calibration of echelle spectra. The spectra obtained with SOFIN typically have $S/N \sim 100$ in the spectral regions of the Mg I and Mg II lines. In the FOCES spectra the S/N depends on the spectral region but in general they are good, ranging from ~ 50 in the bluest part to more than 200 at ~ 8000 Å. The main difficulty in the extraction of the spectra in the Mg II region is the blend with telluric H_2O lines, which are quite numerous near the 7877 Å Mg II line. In order to remove these lines, several rapidly rotating B-type stars were observed as

² Due to not perfect seeing conditions and in order to gain light, for some stars observed with SOFIN we used a slightly larger slit. In this case the resolving power achieved was lower than the quoted value.

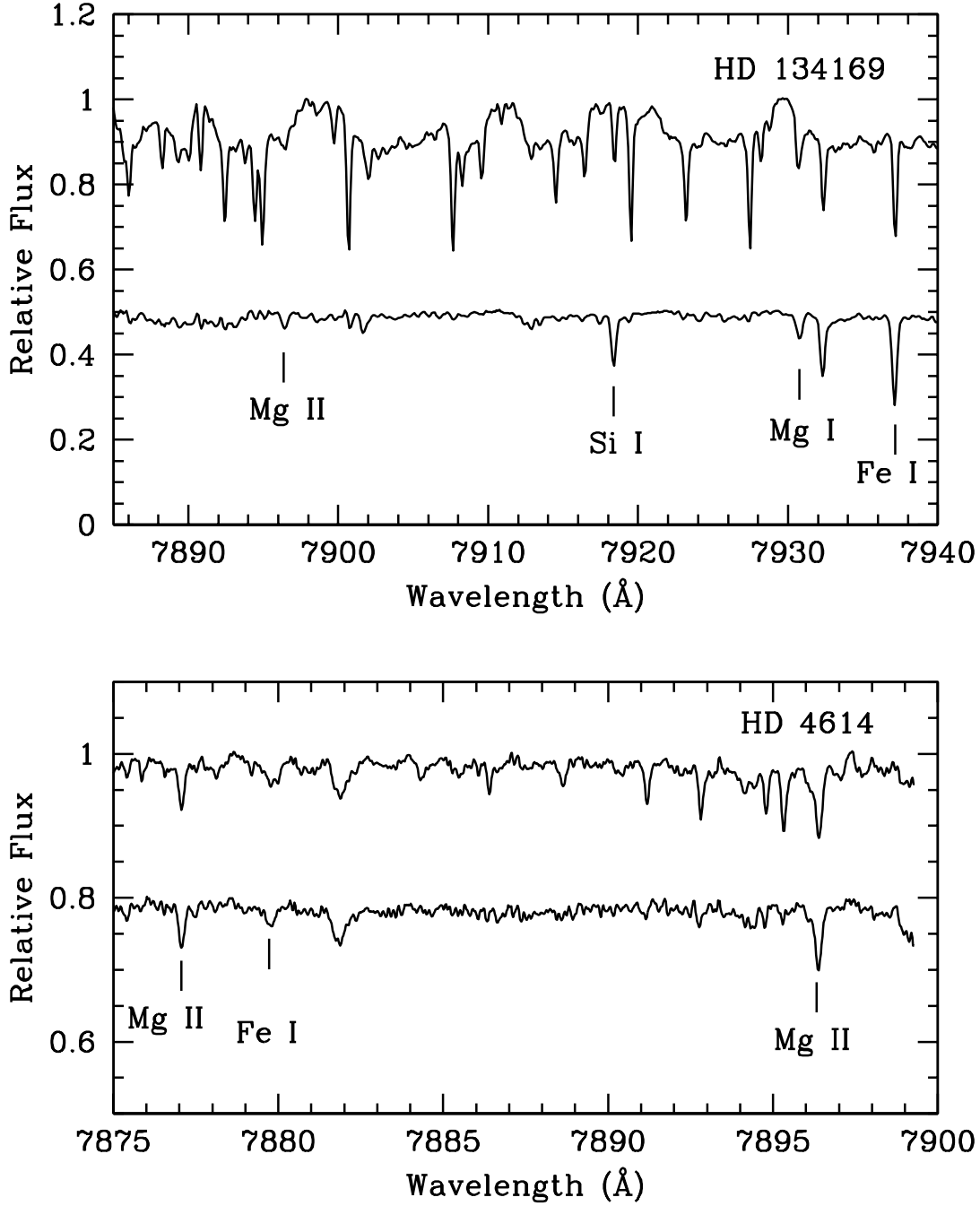


Figure 1. Representative spectra in the region of the Mg II lines before removing the telluric lines (upper spectrum) and after (lower spectrum), respectively. The lower spectrum in each panel has been shifted for clarity. Note the different spectral range and ordinate scale in the plots. The spectra shown also have different spectral resolution. The spectrum of HD 134169 was obtained with FOCES, while HD 4614 with SOFIN. In HD 134169 the Mg II 7877.059 Å line was not detected since due to the radial velocity of the star, the line was placed near the border of the detector. The Mg I 7930.819 Å, however, is clearly seen in this star. This line served as a test to check the telluric line removal procedure (see text).

close as possible in the sky with respect to the target star. We used the IRAF task *telluric* to optimise the fit between the telluric lines of the program star and the hot star by allowing a relative scaling in airmass and wavelength shift. The procedure worked well in most of the stars, but in some cases, the hot-type star could not be observed very close in time and in the sky to the program star. Small *spike* features appeared in these cases in the final spectrum, probably indicating a non-perfect scaling of the airmass. The procedure of telluric absorptions removal certainly adds an extra uncertainty in the derivation of magnesium abundance from the Mg II lines. We realized that when the S/N ratio of both the target and the hot star spectra were not very high, the clean spectrum sometimes had an ill-defined continuum, which translates into a larger error in the equivalent width measurement of the lines. In fact, in some of the stars we derived only upper limits (see below). Figure 1 shows two representative spectra in the region of the Mg II lines before and after the removal of the telluric lines.

3 STELLAR PARAMETERS AND SPECTROSCOPIC DATA

The near infrared Mg II lines are weak, even in solar metallicity stars. This limited the metallicity range of the program stars studied. In fact, theoretical simulations show that for stars with $[\text{Fe}/\text{H}] < -2$, the expected equivalent width in the most favourable cases ($T_{\text{eff}} > 6000$ K and $\log g < 4.0$) of the stronger of the two Mg II lines (7896 Å), would not exceed $\sim 5 - 6$ mÅ, even assuming a typical enhancement $[\text{Mg}/\text{Fe}] \sim +0.4$ dex for a star of this metallicity. The difficulty in detecting such a weak spectral feature is obvious, and is more so when it might be affected by telluric absorptions (e.g. it becomes highly difficult to place the continuum). We decided, hence, to concentrate on the metallicity range $-1.0 \lesssim [\text{Fe}/\text{H}] \lesssim 0.0$, although this, unfortunately, limits our conclusions.

An important issue in abundance analysis is the derivation of the effective temperature. Ideally, one should use an indicator that is insensitive to errors in reddening and to other stellar parameters such as gravity. Theoretically, the profiles of Balmer lines satisfy these conditions, but we could not use them because they were located at the border of the CCD in the echelle spectra, which meant that in many cases their wings were truncated. Therefore, the effective temperature was derived from the $b - y$ and $V - K$ colour indexes using the infrared flux method calibrations of Alonso et al. (1996). The Strömgren photometry was taken from Schuster & Nissen (1988) while K photometry was that of Carney (1983), Alonso et al. (1994) and The Two Micron All Sky Survey (Finlator et al. 2000). According to the *Hipparcos* parallaxes, the majority of our stars are within 100 pc of the Sun, where interstellar reddening is negligible. In any case, the $(b - y)_0$ calibration of Schuster & Nissen (1989) was used to derive interstellar reddening excess. Reddening was only considered for stars with $E(b - y) \gtrsim 0.02$, and the V and K magnitudes, and the m_1 and c_1 indexes were corrected according to the relations with $E(b - y)$ given in Nissen et al. (2002). Photometric values are shown in Table 1. The T_{eff} calibrations by Alonso et al (1996) present little dependency on metallicity, and so it was necessary to estimate a

metallicity value in advance in order to derive T_{eff} . As a first estimate, we took the average metallicity value given in the compilation by Taylor (2003). In general, this metallicity agreed well with the spectroscopic value derived from Fe II lines (see below). When photometry was available, we adopted the mean value of $T_{\text{eff}}(b - y)$ and $T_{\text{eff}}(V - K)$. Both T_{eff} estimates were in agreement within ± 50 K. For the stars with no K photometry, we took the $T_{\text{eff}}(b - y)$ value. Uncertainties in the photometry, reddening and the calibration of the absolute flux in the infrared mainly determine the error in T_{eff} . Alonso et al. (1996) estimated an uncertainty of ± 90 K, taking into account both systematic and random errors in the calibration. Thus, we adopt a conservative error of ± 100 K in T_{eff} .

Gravities were derived from the classical relation

$$\log g/g_{\odot} = \log M/M_{\odot} + 4 \log T_{\text{eff}}/T_{\text{eff}\odot} + 0.4 (M_{\text{bol}} - M_{\text{bol}\odot})$$

taking a value of $M_{\text{bol}\odot} = 4.75$ for the Sun. Absolute visual magnitudes M_V were determined on the basis of *Hipparcos* parallaxes. All parallaxes in the sample stars have an accuracy of $\sigma(\pi)/\pi < 0.3$, and the overwhelming majority < 0.02 . To compute M_{bol} , the bolometric corrections by Alonso et al. (1995) were used. Finally, the stellar mass was derived by interpolating in the $\log L/L_{\odot}$ vs. $\log T_{\text{eff}}$ relation between the α -element enhanced evolutionary tracks by VandenBerg et al. (2000). Depending on the metallicity of the star, we used the tracks computed with different values of the helium fraction Y (from ~ 0.24 to 0.28). The precision in the theoretical derivation of the mass was estimated in $\pm 0.05 M_{\odot}$. The error of the derived value of $\log g$ is mainly determined by the error in M_V (M_{bol}) which is dominated by the uncertainty of the parallax. The estimated final error for $\log g$ ranges from 0.03 to 0.15 dex.

The microturbulence parameter was derived using the relation from Reddy et al. (2003) obtained by studying 33 well defined Fe I lines in 87 dwarf stars with effective temperatures in the range 5650 to 6300 K, $\log g$ from 3.6 to 4.5 and metallicity $-0.8 \lesssim [\text{Fe}/\text{H}] \lesssim +0.1$. The metallicity of three stars in our sample is a little lower than this range, but we believe the expression can be safely used for the entire sample since the use of relatively weak lines makes the abundance analysis almost insensitive to errors in the microturbulence parameter. The relation is

$$\xi_t = 1.28 + 3.3 \times 10^{-4} (T_{\text{eff}} - 6000) - 0.64 (\log g - 4.5)$$

The *rms* error in the least-squares fit derived by these authors is $\sigma \sim 0.15 \text{ kms}^{-1}$. Similar linear regressions have been used by others (Edvardsson et al. 1993; Chen et al. 2000), giving similar results within $\pm 0.25 \text{ kms}^{-1}$, and showing little or no dependence on metallicity as long as weak lines are used (see also Fuhrmann 1998). As a check, we compared our microturbulence values with those spectroscopically derived in works with stars in common. With respect to the work by Gratton et al. (1996) we found a difference of $+0.04 \pm 0.21 \text{ kms}^{-1}$ (6 stars in common), $-0.08 \pm 0.15 \text{ kms}^{-1}$ with Edvardsson et al. (1993, 13 stars) and $+0.19 \pm 0.11 \text{ kms}^{-1}$ with Fuhrmann (2004, 7 stars). Thus, we also adopt a conservative uncertainty in the microturbulence of $\pm 0.25 \text{ kms}^{-1}$. In fact, variations of this amount are unimportant as far as the abundance analysis is concerned, except for the relatively strong Fe II lines at 5197 and 5234 Å in the near solar metallicity stars of our sample (see below).

Table 1. Strömgren photometry, colour excess, $(V - K)$ index and absolute visual magnitude derived from Hipparcos parallaxes for the sample stars. Masses are derived from interpolation in theoretical isochrones $\log L/L_{\odot}$ vs. $\log T_{\text{eff}}$ (see text). The spectrograph used in the observations is indicated.

Star ^a	Instrument	S/N ^b	V_o	$(b - y)_o$	m_o	c_o	β	$E(b - y)$	$(V - K)_o$	M_V	M/M_{\odot}
HD 400	FOCES	80	6.08	0.350	0.141	0.389	2.615	-0.019	...	3.67	1.20
HD 4614	SOFIN	110	3.45	0.402	0.185	0.275	2.588	-0.030	1.480	4.57	1.05
HD 19994	SOFIN	120	5.06	0.361	0.185	0.422	2.631	-0.007	...	3.31	0.95
HD 51530	SOFIN	80	6.20	0.359	0.137	0.401	2.602	-0.014	1.395	2.82	1.20
HD 59984	SOFIN	100	5.90	0.360	0.123	0.336	2.594	-0.004	...	3.51	1.00
HD 106516	FOCES	230	6.10	0.331	0.114	0.334	2.618	-0.012	1.203	4.33	0.90
HD 116316	FOCES	80	7.67	0.316	0.120	0.381	2.630	-0.012	1.211	4.06	1.00
HD 134169	FOCES	275	7.68	0.373	0.119	0.312	2.582	-0.003	1.426	3.80	1.10
HD 150177*	FOCES	330	6.32	0.331	0.119	0.395	2.613	+0.002	...	3.13	1.20
HD 165908	FOCES	660	5.04	0.353	0.135	0.322	2.611	-0.002	...	4.06	0.90
HD 170153	FOCES	214	3.58	0.336	0.146	0.317	2.611	-0.025	...	4.07	1.05
HD 192718	FOCES	158	8.39	0.396	0.144	0.303	2.573	-0.015	...	4.57	0.93
HD 201891	FOCES	295	7.37	0.361	0.094	0.261	2.586	+0.001	1.397	4.62	0.90
HD 207978	FOCES	286	5.55	0.301	0.122	0.425	2.640	-0.002	1.210	3.33	1.05
HD 208906*	FOCES	350	6.95	0.355	0.122	0.292	2.605	-0.012	1.402	4.61	0.97
HD 210595	FOCES	192	8.60	0.305	0.101	0.494	1.222	2.62	1.30
HD 210752	FOCES	195	7.40	0.377	0.132	0.290	2.585	-0.016	...	4.52	1.00
HD 215257*	FOCES	238	7.46	0.358	0.116	0.310	2.594	-0.001	1.530	4.33	0.90
BD +18° 3423	FOCES	122	9.79	0.357	0.090	0.319	2.583	-0.007	1.440	4.54	0.95

^a In the stars marked with an asterisk, the removal of the telluric lines in the Mg II region might be imperfect.

^b Average signal to noise ratio achieved in the spectral region of the Mg II lines.

Table 1 also shows the stellar masses derived, and the final values of T_{eff} , $\log g$ and microturbulence are given in Table 2, together with the values of $[\text{Fe}/\text{H}]$ derived from Fe II lines (see Sect. 3.1). As the calibration of T_{eff} and $\log g$ depends somewhat on $[\text{Fe}/\text{H}]$, the determination of the atmosphere parameters was an iterative process. Comparison between our estimates of T_{eff} and gravity with those derived by authors using different methods shows good agreement. We found mean differences of -13 ± 77 K (Gratton et al. 1996), -73 ± 67 K (Edvardsson et al. 1993) and -73 ± 57 K (Fuhrmann 2004) for the effective temperature in the sense of our values minus theirs, whereas for gravity, -0.07 ± 0.15 (Edvardsson et al. 1993), -0.07 ± 0.15 (Gratton et al. 1996) and $+0.025 \pm 0.060$ (Fuhrmann 2004). Thus, for the adopted uncertainty in T_{eff} and $\log g$, our stellar parameters are well within 1σ with respect to the above studies.

3.1 Stellar metallicity

The derivation of the stellar metallicity measured commonly by the $[\text{Fe}/\text{H}]$ ratio is a critical issue in studying the behaviour of any abundance ratio $[\text{X}/\text{Fe}]$ vs. $[\text{Fe}/\text{H}]$. Here, however, we are mainly interested in the search for systematic differences between Mg I and Mg II abundances and thus any error in $[\text{Fe}/\text{H}]$ would have no greater consequences than a similar systematic effect on the $[\text{Mg}/\text{Fe}]$ ratio derived from Mg I and Mg II lines.

Thévenin & Idiart (1999) showed that departures from N-LTE of Fe I lines may lead to systematic errors in the derivation of the metallicity in metal-poor stars. N-LTE metallicity corrections can reach up to 0.35 dex, and are thus, not negligible. However, Korn et al. (2003) recently showed that this result depends crucially on the choice of

Table 2. Stellar parameters

Star	$T_{\text{eff}}(\text{K})$	$\log g$	$\xi(\text{kms}^{-1})$	$[\text{Fe}/\text{H}]$
HD 400	6147	4.15	1.55	-0.17
HD 4614	5790	4.34	1.31	-0.35
HD 19994	6030	3.90	1.67	+0.18
HD 51530	5910	3.75	1.73	-0.43
HD 59984	5871	3.91	1.61	-0.77
HD 106516	6105	4.40	1.38	-0.85
HD 116316	6195	4.24	1.51	-0.67
HD 134169	5806	4.00	1.54	-1.00
HD 150177	6084	3.91	1.68	-0.73
HD 165908	5924	4.10	1.51	-0.67
HD 170153	6030	4.21	1.48	-0.68
HD 192718	5787	4.28	1.35	-0.66
HD 201891	5842	4.30	1.35	-1.10
HD 207978	6270	4.00	1.68	-0.66
HD 208906	5875	4.31	1.37	-0.76
HD 210595	6256	3.80	1.81	-0.64
HD 210752	5847	4.31	1.35	-0.65
HD 215257	5890	4.21	1.43	-0.72
BD +18° 3423	5891	4.31	1.36	-0.93

the neutral hydrogen collision scaling factor (S_H) (Thévenin & Idiart did not consider this). For a value of $S_H = 3$ and using effective temperatures derived from fitting the Balmer profiles, they found excellent consistency between the metallicity derived from both Fe I and Fe II lines in a small sample of metal-poor stars. Nevertheless, the role of hydrogen collisions in keeping LTE in metal-poor atmospheres is still a matter of debate (cf. Barklem et al. 2003) (in fact Korn et al. 2003, did not find any physical reason to justify $S_H = 3$). Thus, because iron abundances based on Fe II lines do not

Table 3. Fe and Mg lines used in this study, showing equivalent widths as measured in the solar flux spectrum together with the abundances derived for each line

Wavelength (Å)	χ (eV)	$\log gf$	Sun W_{λ}^{\odot} (mÅ)	$\log \epsilon(X)^a$
Fe II				
5100.66	2.81	-4.19	19.6	7.50
5197.58	3.23	-2.28	88.4	7.40
5234.62	3.22	-2.20	90.5	7.53
5325.55	3.22	-3.27	43.0	7.50
5414.08	3.22	-3.80	27.0	7.58
5425.26	3.20	-3.42	44.0	7.60
6084.10	3.20	-3.86	21.3	7.55
6149.25	3.89	-2.77	38.0	7.54
6247.56	3.89	-2.38	56.2	7.57
6416.93	3.89	-2.79	42.2	7.67
6432.68	2.89	-3.76	43.0	7.68
6456.39	3.90	-2.13	66.5	7.55
Mg I				
4571.096	0.00	-5.610	110	7.50
4730.029	4.34	-2.150	77	7.49
5528.409	4.34	-0.498	300	7.60
5711.091	4.34	-1.810	106	7.50
6318.750	5.10	-1.970	43	7.55
7930.810	5.94	-1.300	59	7.65
Mg II				
7877.054	9.99	+0.390	15	7.62
7896.390	9.99	+0.650	21	7.60

^a Abundances are given in the scale $\log N(H) \equiv 12$.

suffer important N-LTE effects, we based the derivation of metallicity on the analysis of a number of relatively weak and unblended Fe II lines. The list of lines is given in Table 3, and is almost the same as that used by Nissen et al. (2002). The gf -values for these lines are from Biémont et al. (1991) (see Nissen et al. 2002 for more details). To minimise systematic errors due to wrong gf values, we performed a relative analysis with respect to the Sun, line-by-line; thus, the iron abundance in the Sun was considered as a free parameter. We adopted the Unsöld (1955) approximation to the van der Waals damping constant with an enhancement of $\log \gamma_6$ by a factor of 2.5. Except for the Fe II lines at 5197 and 5234 Å in the stars of the sample with largest metallicity (HD 400, HD 4614 and HD 19994), iron abundance is practically independent of the damping parameter as well as of the microturbulence parameter. In fact, no correlation was found between the Fe abundance and the equivalent widths of the lines in any star. By using Kurucz’s model atmosphere for the Sun with parameters 5780 K, $\log g = 4.44$ and $\xi_t = 1.15 \text{ km s}^{-1}$, and the equivalent widths of the Fe II lines as measured in the solar flux spectrum (Kurucz et al. 1984), the average solar abundance derived was $\log \epsilon(\text{Fe}) = 7.54$, very close to the commonly adopted meteoritic value of 7.50 (Grevesse & Sauval 1998)³. The relatively large iron abundance scatter

found in the Sun (± 0.08 dex, see Table 3) is probably due to errors in the gf -values. However, this problem is avoided by working differentially line-by-line with respect to the Sun in the sample stars. The iron line scatter found in the program stars ranges from ± 0.07 to ± 0.12 dex. On the other hand, the error induced by the uncertainty in T_{eff} (± 100 K) is typically less than ± 0.07 dex, while an error in $\log g$ (± 0.15) introduces an error of about ± 0.06 dex into $[\text{Fe}/\text{H}]$. By adding these errors (quadratically) to the error due to line-to-line scatter from the equivalent width measurements, we derive a typical error of ± 0.10 dex for $[\text{Fe}/\text{H}]$. The error may be a little larger (± 0.13 dex) when the 5197 and 5234 Å Fe II lines are considered individually because of their sensitivity to microturbulence.

The literature contains a large number of studies with stars in common, with which our estimate of metallicity can be compared. Note that our metallicities agree to better than ± 0.10 dex with the recommended value given in Taylor’s (2003) metallicity compilation. A better criterion is to compare our results with those obtained in similar studies. Com-

into account N-LTE and the effect of granulation in the formation of Fe I and Fe II lines found a lower value, $\log \epsilon(\text{Fe}) = 7.45 \pm 0.05$ (Aplund et al. 2000; Bellot-Rubio & Borrero 2002). Nevertheless, in this paper we adopt the solar abundances cited by Grevesse & Sauval except where explicitly mentioned.

³ Recent abundance studies in the solar photosphere which take

parison with the N-LTE $[\text{Fe}/\text{H}]$ values given in Thévenin & Idiart (1999) shows a mean systematic difference -0.15 dex (in the sense of our results minus theirs) which can be explained by the differences in the stellar parameters adopted (effective temperature and gravity). With respect to the studies mentioned above, in comparing temperatures and gravities, the comparison of stars in common shows a mean difference in $[\text{Fe}/\text{H}]$ of -0.023 ± 0.14 , -0.04 ± 0.11 and -0.05 ± 0.07 with Gratton et al. (1996), Edvardsson et al. (1993) and Fuhrmann (2004), respectively. Note again that systematic errors in $[\text{Fe}/\text{H}]$ would affect the $[\text{Mg}/\text{Fe}]$ ratios derived from Mg I and Mg II lines in the same sense. The final metallicities derived are shown in Table 2.

3.2 The magnesium lines

Table 3 also shows the list of magnesium lines used in this study. Except for the 7930 Å line, the remaining lines are widely used in the literature. They are catalogued as *clean* lines by Lambert & Luck (1978) although the 4730 Å line could be affected by a Cr I line at 4729.859 Å and the 6318 line by the middle line belonging to the Mg triplet between 6318-6319 Å. Due to its proximity to the Mg II lines, the Mg I 7930 Å served as an indirect test of the method of telluric absorption removal in this region (see below). The *gf*-values for the Mg I lines were taken from Wiese et al. (1969) and Kurucz & Peytremann (1975). They agree quite well with other accurate lifetime measurements (Kwong et al. 1982; Lambert & Luck 1978, and references therein). The van der Waals damping constants adopted are those deduced by Zhao et al. (1998) from the N-LTE analysis of several neutral magnesium lines in the solar atmosphere, except that for the 7930 Å line, where we adopted the classical Unsöld constant with an enhancement by a factor of 2.5. The *gf*-value for this line is rather uncertain, as it seems to be formed by several (crowded) Mg I absorptions. In fact, in the solar spectrum this line shows an asymmetry to the red. We used the *gf*-value deduced by Thévenin (1990) from the solar spectrum. In the VALD database (Kupka et al. 1999) there appears a Ca I line at 7930.851 Å that may contribute to the 7930 Å Mg I feature. However, we found that even in the Sun its contribution is negligible (< 0.2 mÅ).

As for iron, we preferred to keep the solar magnesium abundance free and to carry out a line-by-line relative analysis with respect to the Sun. This should minimise systematic errors due to uncertain *gf*-values. As can be seen in Table 3, using Kurucz’s model atmosphere for the Sun, the average magnesium abundance derived from Mg I lines is $\log \epsilon(\text{Mg}) = 7.530 \pm 0.035$ which is in good agreement with the photospheric magnesium abundance (7.58 ± 0.05 , Grevesse & Sauval 1998). Using the Howelger & Müller (1974) model for the Sun, a closer figure to the photospheric value is found, namely $\log \epsilon(\text{Mg}) = 7.568 \pm 0.019$. We believe this is evidence of reliable *gf*’s. Spectroscopic data for the Mg II lines are from the VALD database. In this case, we also adopted the standard van der Waals damping constant, multiplied by a factor of 2.5. Systematic differences between the Mg I and Mg II abundances due to differences in the damping constant should be unimportant in a relative analysis, because of the weakness of the Mg lines in our stars. Also, the average solar magnesium abundance obtained from Mg II lines agrees with the solar value obtained by Grevesse & Sauval.

Let us now discuss the effect on the abundances of the errors in the equivalent widths and model atmosphere parameters. Errors affecting the derived abundances of Mg vary from line to line, although obviously this does not put into question the validity of the LTE approach (however, see below). Cayrel (1988) gives a method to evaluate the error in the equivalent widths

$$\Delta W_\lambda = \frac{1.6\sqrt{w\delta x}}{S/N}$$

where w is the FWHM of the line, δx is the pixel size in Å, and S/N the signal-to-noise ratio per pixel in the continuum. In our spectra, these parameters are different for FOCES and SOFIN and for a given instrument, the S/N ratio also varying from the blue orders to the red ones. Moreover, the error in the equivalent widths is larger than that derived from this formula when it is applied to the Mg II lines because of the extra uncertainty introduced in the position of the continuum when telluric absorptions are removed. In this case, the uncertainty of the continuum position may reach a maximum of 1-2%. For the Mg II lines and in the case of FOCES spectra, we estimate $\Delta W_\lambda \sim 2-4$ mÅ, while for those obtained with SOFIN, $\sim 0.5-3$ mÅ, depending on the S/N of the spectrum. Certainly, the error is lower for the Mg I and Fe II lines, which are not affected by telluric absorptions. Table 4 shows the sensitivity of the Mg abundances to the uncertainties in the model atmosphere for each Mg line, as well as for an uncertainty of ~ 2 mÅ in the equivalent width as a representative case. The table is constructed using the atmosphere parameters of a typical star in the sample, namely $T_{\text{eff}} = 5900$ K, $\log g = 4.00$, $\xi_t = 1.50 \text{ km s}^{-1}$ and $[\text{Fe}/\text{H}] = -0.6$. It is clear that the total error is dominated by the uncertainty in the effective temperature and gravity. This is particularly evident for the Mg II lines, which are also significantly affected by errors in the equivalent width measurement.

The last column in Table 4 indicates the total error estimated assuming that the effects of all these errors on Mg abundance are uncorrelated.

An important issue is how to compute the average magnesium abundance derived from the neutral lines for comparison with Mg II abundances. We did not find any objective reason to discard any of the Mg I lines. Thus, we decided to compute the average Mg I abundance by weighting the abundances from each line according to the total formal error shown in the last column of Table 4, namely

$$\log \epsilon(\text{Mg}) = 1/v \sum_i (\epsilon_i/\sigma_i)$$

where v is the statistical variance, and ϵ_i and σ_i are the Mg abundance and the total formal error from each line (see Table 4). For the Mg II abundance, we derived the mean value of the two lines.

Before comparing the magnesium abundances obtained with earlier studies and between the different magnesium indicators, we should consider the effects of departures from LTE in both the Mg I and the Mg II lines.

3.2.1 N-LTE effects on Mg lines

Departures from LTE of neutral lines of Mg have been widely studied in the literature. Starting with the analysis by Athay

Table 4. Effects on LTE magnesium abundances of changing atmosphere parameters for each spectral line used. A representative case is shown.

line	$\Delta T_{\text{eff}} = \pm 100 \text{ K}$	$\Delta \log g = \pm 0.15$	$\Delta \xi = \pm 0.25 \text{ km s}^{-1}$	$\Delta [\text{Fe}/\text{H}] = \pm 0.10$	$\Delta W_{\lambda} = \pm 2 \text{ m\AA}$	Total
Mg I 4571	± 0.12	∓ 0.010	∓ 0.035	± 0.010	± 0.03	± 0.14
Mg I 4730	± 0.06	∓ 0.015	∓ 0.010	± 0.005	± 0.04	± 0.08
Mg I 5528	± 0.07	∓ 0.070	∓ 0.025	± 0.025	± 0.01	± 0.13
Mg I 5711	± 0.05	∓ 0.030	∓ 0.020	± 0.040	± 0.02	± 0.11
Mg I 6318	± 0.05	∓ 0.005	∓ 0.000	± 0.010	± 0.08	± 0.11
Mg I 7930	± 0.04	∓ 0.005	∓ 0.000	± 0.000	± 0.08	± 0.12
MgII 7877	∓ 0.09	± 0.05	∓ 0.00	± 0.00	± 0.15	± 0.18
MgII 7896	∓ 0.08	± 0.04	∓ 0.00	± 0.00	± 0.15	± 0.17

& Canfield (1969) in the solar photosphere, all the subsequent works (Mauas et al. 1988; Mashonkina et al. 1996; Zhao et al. 1998; Zhao & Gehren 2000 etc) agree concerning the conclusions: N-LTE effects are quite small in the Sun for most Mg I lines in optical wavelengths. For metal-poor dwarf stars, departures from LTE increase due to photoionisation predominating over collisions. The reduction of gravity reduces the efficiency of the collisions, and hence a decrease in the stellar gravity also tends to increase N-LTE effects. As a rule, the lower the metallicity and gravity and the higher the effective temperature, the greater the effects of N-LTE on Mg I lines. However, for the stellar parameters of the stars studied here, N-LTE corrections (positive) to Mg I abundances do not exceed +0.15 dex. Unfortunately, the literature does not contain detailed N-LTE calculations for all the Mg I lines studied here. Thus, we could only correct the Mg I LTE abundances for cases in which specific calculations were available. We used the N-LTE calculations by Zhao & Gehren (2000) for the Mg I lines at 4571, 4730, 5528 and 5711 Å, interpolating from their Table 1 for the stellar parameters of our stars. The Mg I N-LTE corrections by Zhao & Gehren are based on the assumption of a common turbulence. However, when the corrections are not very large, as is the case in question, they do not depend on the turbulence (at least within 0.01-0.02 dex). Our N-LTE Mg I abundances are derived using only the N-LTE abundances from these four lines, as indicated above.

To the best of our knowledge, the literature does not contain N-LTE studies of the Mg II lines in cool stars. However, several analyses of kinetic equilibrium of Mg II exist for hot stars (Mihalas 1972; Sijnders & Lamers 1975; Sigut & Lester 1996; Przybilla et al. 2001). Here, we make use of the main results of these studies. In the atmosphere of cool stars, Mg II is the majority species ($N(\text{Mg II})/N(\text{Mg I}) \geq 10^3$). Two useful consequences follow from this; first, bound-bound ($b-b$) and bound-free ($b-f$) transitions in Mg I have a negligible effect on the kinetic equilibrium of Mg II and thus, Mg I levels can be ignored in the atom model. In any case, here we considered five of the lowest terms of Mg I only for number conservation. Second, as shown in previous studies where ions comprised the majority species (e.g. Ba II, Mashonkina et al. 1999; Cl, Ni, and OI, Takeda 1994), departures from LTE for Mg II are expected to be caused mainly by radiative $b-b$ transitions. Thus, one may disregard the strong coupling of Mg II to the Mg III continuum. For this reason, we include all the levels of Mg II up to $n = 12$ in the atom model, leaving a gap of 0.3 eV before

the Mg III continuum. All levels with $l \geq 4$ were further collapsed into the ^2G levels. Levels for $n = 11$ and 12 were treated as single hydrogen levels. The multiplet structure of all levels was ignored. The final atom model includes 35 levels of Mg II and the ground state of Mg III. We used laboratory energy levels collected by Sigut & Lester (1996) as shown in their Table 1.

The oscillator strengths for the 284 allowed transitions were compiled from a variety of sources. For the $3s - np$ series, $n = 3 - 6$, f -values were taken from the close-coupling calculations by Butler et al. (1984). For transitions between the states $3p, 4s, 4p, 5s, 5p$ and $6s$, we adopted the results of Hibbert et al. (1983). For the remaining transitions between states with $n \leq 10$ and $l \leq 3$, the data from the TOPBASE database (Cunto et al. 1993) were used. The remaining f -values were computed using the Coulomb approximation following Oertel & Shomo (1968). The close-coupling results of Butler et al. (1984) were adopted for the photoionisation cross section of the Mg II ground state. The remaining photoionisation cross sections for $l \leq 3$ were taken from Hofsaess (1979). Sigut & Lester (1996) compared these data with the recent Opacity Project results available through the TOPBASE database and found that the low excited level cross sections agree within 10% at threshold. Considering the insignificant role played by $b-f$ transitions in producing departures from LTE for Mg II (see below), such uncertainty does not affect the final results. The hydrogenic photoionisation cross sections with $Z = 2$ were adopted for $l \geq 4$.

In cool stars the ratio of electrons to hydrogen atoms determines the importance of both types of inelastic collisions. Drawin's (1968) formula, as described by Steenbock & Holweger (1984), is widely used to calculate hydrogenic collisions, and it suggests that their influence is comparable with that of electron impacts⁴. In our calculations we take into account both types of collisions. Collision strengths Ω for electron excitation among the lower states of Mg II, up to and including $5p$, were taken from close-coupling calculations of Sigut & Pradhan (1995). The remaining collisional rates were calculated using the formula of van Regemorter (1962) for allowed transitions, and that by Allen (1973) with $\Omega = 1$, for forbidden ones. For inelastic collisions with neu-

⁴ However, a recent study of the inelastic collision of Li + H (Barklem et al. 2003) shows that Drawin's formula typically greatly over-estimates the collisions with hydrogen.

tral hydrogen, we use the formula of Steenbock & Holweger (1984). Since this formula provides only an order of magnitude estimate, the cross-sections were multiplied by appropriate scaling factors S_H in order to produce the best fit to the solar Mg II level populations and line profile of the Mg II 7896 Å line⁵. Collisional ionisation by electrons was treated following Seaton's formula as described by Mihalas (1978), in which the collisional ionisation rate is taken to be proportional to the photoionisation cross section.

The Mg II kinetic equilibrium was calculated using the code NONLTE3 (Sakhibullin 1983), based on the complete linearization method described by Auer & Heasley (1976). The method of calculation was up-dated including a new opacity package. In the new version, we used the formulae and atomic data from ATLAS9 by Kurucz (1998) to compute $b-f$ and $f-f$ transitions of H, H^- , H_2^+ and He I, $b-f$ transitions of neutral atoms and the first ions of the most abundant elements, the H I line opacity, Rayleigh scattering and electron scattering. Furthermore, the background opacity includes the molecular absorption from 11 of the most abundant molecules and line absorptions. The line opacity due to the metals was explicitly included in the calculations. The metal line list was extracted from the Kurucz (1998) compilation and contains about 152000 lines of neutral atoms and the two first ionisation stages between 91.2 and 10000 nm. Wavelengths of the Mg II $b-b$ transitions are not calculated from level energies but are given in correspondence with the metal line list to correctly account for the background line opacity. The radiative $b-b$ rates were treated with a Voigt profile. The natural width of each line was computed using the classical damping constant, while the van der Waals damping was obtained using the values indicated above. The Stark width for the resonance transition $3s-3p$ was taken from the close-coupling calculations of Barnes (1971) and for the remaining transitions we used the formulae $\gamma_4 = 2 \times 10^{-8} n_e n_{eff}^5$, where n_e is the electron number density and n_{eff} is the effective quantum number.

For T_{eff} and $\log g$ values close to the solar ones, the kinetic equilibrium of Mg II is mainly affected by radiative processes in $b-b$ transitions, because this is the dominant ionisation state. In Figure 2, the departure coefficients, $b_i = n_i^{N-LTE}/n_i^{LTE}$, of the few important Mg II levels as a function of continuum optical depth τ_{5000} are shown for a typical atmosphere of the star sample ($T_{eff} = 6105$ K, $\log g = 4.23$ and $[M/H] = -0.85$). Here, n_i^{N-LTE} and n_i^{LTE} are the N-LTE and thermal (Saha-Boltzmann) number densities, respectively. No process seems to affect the Mg II ground state population, and $3s$ maintains its thermodynamic value. The departure coefficients of all the excited levels begin to deviate from 1 at depths around $\log \tau_{5000} = 0.25$, where photon losses in the resonance line wings start to become important. Overpopulation of the excited levels $3p$, $4s$ and $3d$ inside $\log \tau_{5000} = -1.5$ is produced by the pumping transitions, the resonance transition, $3s-3p$ ($\lambda 2800$ Å), in the first turn, $3p-4s$ ($\lambda 2936$ Å) and $3p-3d$ ($\lambda 2798$ Å). Enhanced excitation of the levels above $3d$ is provided by the close coupling to $4s$ and $3d$ and to each other. The departure coefficients of excited levels start to decrease in

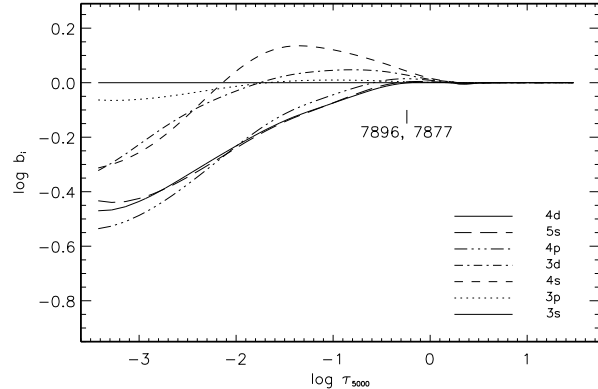


Figure 2. Departure coefficients b_i for some levels of Mg II in the model atmospheres with $T_{eff} = 6105$ K, $\log g = 4.23$ and $[M/H] = -0.85$. Tick marks indicate the locations of line centre optical depth equal to unity for the Mg II lines at 7877 and 7896 Å.

the upper layers ($\log \tau_{5000} < -1$), which are transparent with respect to the radiation of the subordinate lines. From the behaviour of the departure coefficients, we expect the lines at 7877 and 7896 Å of the multiplet $4p-4d$ to be amplified, compared with the LTE case. In the line formation layers $b_{4d} < b_{4p}$ holds, and the source function approaches $S_{4p,4d} \approx b_{4d}/b_{4p} B_\nu(T_e) < B_\nu(T_e)$. In addition, the departure coefficients of the lower level are larger than 1, which strengthens the lines studied here.

Since collisions with neutral hydrogen could affect the kinetic equilibrium of Mg II (see, however, Barklem et al. 2003), we have tried to find their efficiency empirically from the fit to the profile of the Mg II 7896 Å line in the solar spectrum. For the Sun, we compared different atomic models excluding and including collisions with neutral hydrogen using various factors, $S_H = 0.005, 0.01, 0.1$ and 1. Figure 3 shows the results for the Mg II 7896 Å line. All the theoretical profiles were calculated using the oscillator strengths and Mg abundances listed in Table 3. The theoretical profiles were convolved with a profile that combines rotational and macroturbulence broadening with velocities $V_{rot} = 1.8$ km s^{-1} and $V_{mac} = 4.2$ km s^{-1} , respectively. For the sake of comparison, the LTE profile corresponding to the same fitting parameters is also shown. Unfortunately, as noted above, this Mg II line is located in the red wing of a telluric absorption and our calculations cannot reproduce the continuum level correctly (see Figure 3). If hydrogen collisions are small in number ($S_H = 0.005, 0.01$) we obtain slightly broader and deeper theoretical profiles compared with the LTE case. On the contrary, the inclusion of these processes with $S_H = 0.1$ and 1 makes the N-LTE profile shallower and narrower than the LTE one. From Figure 3 we conclude that S_H should be lower than 0.1. In our previous studies, a value of $S_H \sim 0.01$ was derived from analysis of the 10327 Å Sr II line (Mashonkina & Gehren 2001). The present analysis does not contradict the earlier ones and therefore we accept $S_H = 0.01$.

For all the stars in our sample the N-LTE abundance corrections (Δ_{N-LTE}) were calculated for both Mg II lines as the difference between N-LTE and LTE abundances. As ex-

⁵ This is the stronger feature of the two Mg II lines and, in the solar spectrum, is less blended by telluric absorptions.

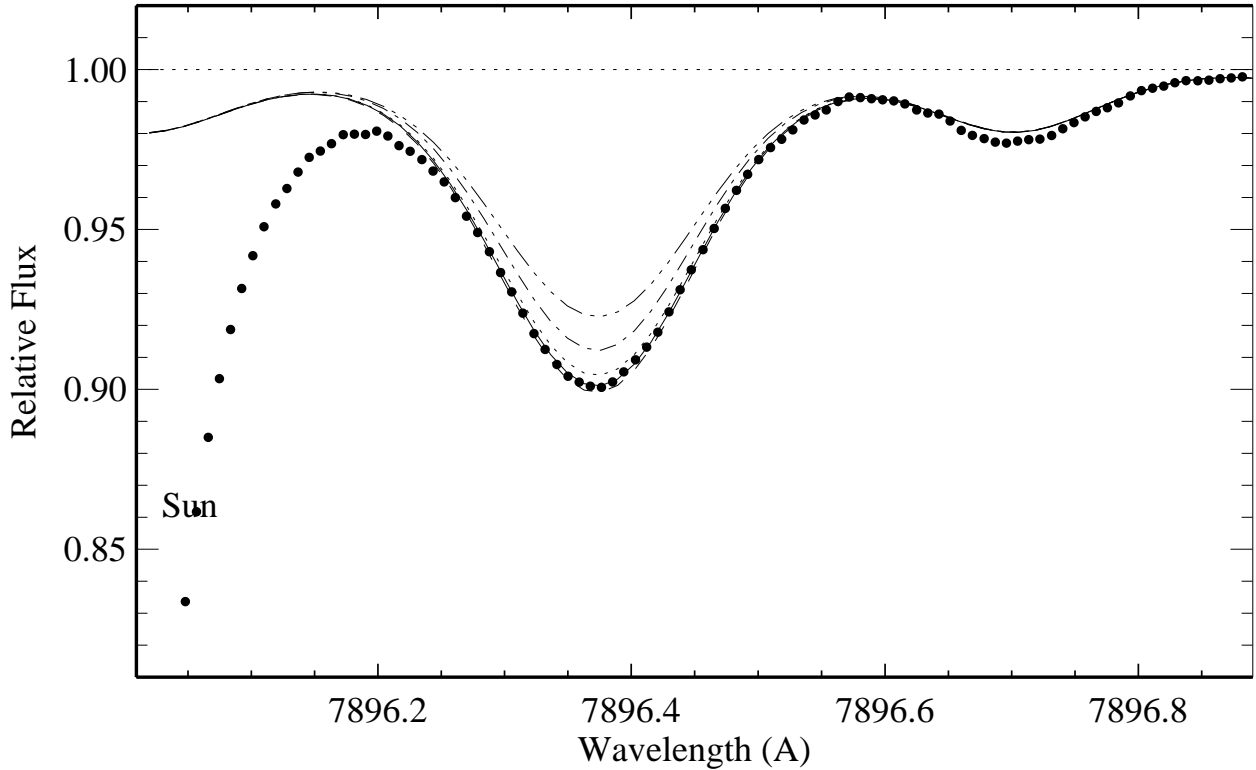


Figure 3. Synthetic N-LTE and LTE flux profiles for the Mg II 7896 Å line compared with the solar flux spectrum (Kurucz et al. 1984) (bold dots). Different lines correspond to LTE (dotted line), $S_H = 0.005$ (dashed line), $S_H = 0.01$ (solid line), $S_H = 0.1$ (dashed-dotted line) and $S_H = 1$ (dashed-three-dotted line). See text for discussion of the fitting parameters.

pected from the behaviour of the departure coefficients, the two Mg II lines are strengthened compared with the LTE case and, for the whole range of stellar parameters investigated, Δ_{N-LTE} is negative. Since, qualitatively speaking, these lines form in quite deep layers, the N-LTE effects are not very large and Δ_{N-LTE} does not exceed 0.07 dex for the 7877 Å or 0.11 dex for the 7896 Å line, respectively. In the Sun, $\Delta_{N-LTE} = -0.02$ and -0.03 dex, correspondingly, with $S_H = 0.01$. In order to evaluate the uncertainty in our N-LTE corrections, for the Sun, we performed test calculations to check the sensitivity when electronic collision rates were varied. Increasing the van Regemorter rates by a factor of 10 with $S_H = 0.0$ has a negligible effect (between 0.004 – 0.006 dex). Finally, since in the atmospheres of cool stars Mg II is a dominant specie, uncertainty in the photonionization cross-section has almost no effect on the final corrections. Note however, that if neutral H collisions had no effect at all on the kinetic equilibrium of Mg II (i.e. $S_H = 0.0$), N-LTE corrections would be more negative. Thus, we consider our N-LTE corrections as lower limits.

4 RESULTS AND DISCUSSION

The abundances from Mg I and Mg II lines were derived by the classical method of interpolating the measured equivalent width in a theoretical growth curve. Such growth curves

were constructed for each line and star from a model atmosphere with the parameters in Table 2 interpolated in the grid of models by Kurucz (1998). The agreement between the different Mg I features is good. For stars where more than two Mg I lines are used (15 stars), we derived a mean dispersion of ± 0.09 dex. This value is of the same order as the formal error expected in the abundances derived from individual Mg I lines (see Table 4). Considering this, we adopted ± 0.12 dex as the typical error in the [Mg I/H] ratios.

Barbuy et al. (1985) and Magain (1989) found discrepancies between the magnesium abundances derived from the resonance intercombination line (4571 Å) and higher excitation Mg I lines in giant and dwarf stars. They suggested N-LTE effects due to overionisation as the cause of these differences, which could reach +0.6 dex. However, Fuhrmann et al. (1995) and Carretta et al. (2000) found a good agreement between the different Mg I line indicators. The same is true when N-LTE corrections are applied, and hence the differences in Mg abundances obtained by Barbuy et al. (1985) and Magain (1989) when using the 4571 Å line must be attributed to another factor. Carretta et al. (2000) suggest the choice of the oscillator strength. We did not find any systematic difference between the intercombination line and the other higher excitation Mg I lines. For instance, the mean difference between the intercombination line and the mean value derived from the 4730, 5528 and 5711 Å

lines is $+0.05 \pm 0.05$. No correlation was found either between this abundance difference and T_{eff} and/or $\log g$. In the same line, we found no systematic differences between the Mg I abundances derived from the different high excitation lines. The mean difference between the 7930-based abundance and that from the 4730, 5528, 5711 and 6318 Å is $+0.02 \pm 0.08$. Again, no correlation was found against the stellar parameters. This would indicate that systematic errors in the derivation of the stellar parameters in our stars are probably minimal. Surprisingly, however, we did find a systematic difference between the 5711 Å line and the other two lines with equal excitation energy, namely the 4730 and 5528 Å lines. This systematic difference is $+0.09$ dex in the sense of the 5711 Å minus the mean value of the other two. We have not found an obvious explanation for this fact. The increase in the T_{eff} values would help eliminate this difference, but not by very much as these three lines show a similar behaviour against T_{eff} variations (see Table 4). We searched for possible unidentified blends at 5711 Å in the data bases of Kurucz and VALD, but no line was found that might produce such an effect. Nor are N-LTE effects the solution, as these are similar for the three lines and are found in the same sense (see Zhao & Gehren 2000). Although this systematic difference is small considering the formal error bar, it merits further study as many works in the literature base their Mg abundances only on the 5711 Å line. On the other hand, the fact that the Mg I abundances derived from the 7930 Å line agree with those obtained from the other Mg I lines gives us some confidence in the method used to remove telluric lines, which may affect the Mg II lines.

Let us now compare our results with those reported from other magnesium abundance analyses in the literature. We have twelve stars in common with the ample study by Edvardsson et al. (1993) in field dwarf stars. Our Mg I based abundances are systematically lower by a factor $+0.10 \pm 0.12$ dex. This can be explained, however, by the differences in the effective temperature and gravity adopted. These authors derive systematically higher temperatures and gravities than found by us (see above). From Table 4, these differences in the stellar parameters easily account for the differences in Mg abundances. In fact, for the four stars in common with these authors where the differences in T_{eff} are less than 50 K, the Mg abundances agree to better than ± 0.05 dex. We also found agreement between error bars with other similar studies, namely mean differences of -0.01 dex with Fuhrmann et al. (1995) (4 stars), $+0.07$ dex with Carretta et al. (2000) (2 stars), $+0.10$ dex with Mashonkina et al. (2003) (1 star) and -0.08 dex with Gratton et al. (2003a) (6 stars). In all cases, the differences can be explained as being due to differences in the stellar parameters.

4.1 Abundances from Mg II lines

Table 5 shows the final $[\text{Mg}/\text{H}]$ ratios derived from the Mg I and Mg II features. The ratios corrected for N-LTE effects according to Section 3 are also shown. Columns 6 and 7 compare LTE and N-LTE Mg abundances in the sense $\Delta[\text{Mg}/\text{H}] = [\text{MgII}/\text{H}] - [\text{MgI}/\text{H}]$, respectively. As can be seen from column 6, the classical LTE abundance analysis gives a very good agreement between the Mg I and Mg II lines, the mean difference being only $\sim +0.02$ dex, although with a significant scatter ($\sim \pm 0.08$ dex) which is, however, compatible

with the expected formal error in the Mg I-II abundances. When applying N-LTE corrections, agreement is also found between Mg I and Mg II although, surprisingly, the mean difference is now larger ($\sim -0.08 \pm 0.09$ dex) and changes of sign⁶. We believe the larger difference between Mg I and Mg II N-LTE abundances is in some way artificial. The question is that our estimated formal error in Mg I and Mg II abundances (see Table 4) in individual stars is, in most cases, much larger than the corresponding N-LTE abundance correction (see Sect. 3). Therefore, in this particular case, considering departures from N-LTE effects does not necessarily improve the agreement between Mg I and Mg II but introduces some *noise*. [Note that ignoring the collisions with neutral hydrogen ($S_H = 0.0$) in the N-LTE calculations on Mg II would slightly enlarge the difference between Mg I and Mg II in the N-LTE case].

In order to test for systematic differences between Mg I and Mg II abundances, we searched for correlations with the stellar parameters. Figure 4 shows that there is no apparent correlation with T_{eff} and/or gravity. Obviously, this should be tested further using a larger sample of stars, spanning a wider range in metallicity.

Figure 5 plots the typical $[\text{Mg}/\text{Fe}]$ vs. $[\text{Fe}/\text{H}]$ relationship obtained from Mg I and Mg II lines. From the discussion above, it is obvious that these diagrams are very similar. Near solar ratios ($[\text{Mg}/\text{Fe}] \approx 0.0$) are obtained in stars with $[\text{Fe}/\text{H}] \gtrsim -0.6$, while for stars with a lower metallicity, a small enhancement is typically found ($[\text{Mg}/\text{Fe}] > 0.0$). Note the increase and/or scatter of the $[\text{Mg}/\text{Fe}]$ ratio near $[\text{Fe}/\text{H}] = -0.6$, independently of the Mg indicator. This effect was also found in other magnesium studies (see references in Sect. 1). Fuhrmann et al. (1995) suggested that this is a consequence of the onset of the Galactic disk formation. More extended analyses (e.g. Edvardsson et al. 1993; Prochaska et al. 2000; Reddy et al. 2003) found a fairly similar feature in the $[\text{Mg}/\text{Fe}]$ ratio at this metallicity, although not as abrupt as that found by Fuhrmann et al. Indeed, differences in the $[\text{Mg}/\text{Fe}]$ ratios are found in metal-poor stars with overlapping metallicity, which is currently interpreted as differences in the star formation history between the Galactic halo, thick and thin disk and/or due to chemical inhomogeneities in the interstellar medium (see e.g. the critical discussion by Fuhrmann 1998). Similar differences between different population stars at a given metallicity seem also to exist in the $[\text{O}/\text{Fe}]$ ratio (Bensby et al. 2003) and in other α -elements, such as Ca and Ti (Prochaska et al. 2000). In our small sample, this effect might also be present. In fact, according to their kinetic properties (T. Borkova, private communication) the stars HD 106516, HD 134169, HD 192718, HD 201891 and HD 208906 in our sample might be considered as members of the thick disk. The remaining stars, except BD +18° 3423 (a halo star; $(U, V, W) = (-83, -264, -50)$, $V_{\text{pec}} = 282 \text{ km s}^{-1}$, $e = 0.89$), probably belong to the thin disk. At the overlapping metallicity of the thick and thin disks ($[\text{Fe}/\text{H}] \sim -0.6$), thick disk stars tend to have higher $[\text{Mg}/\text{Fe}]$ ratios than thin disk stars (Fuhrmann 1998; Gratton et al. 1999). Comparison of the $[\text{Mg}/\text{H}]$ ratio (see Table 5) in the thick disk star HD 192718

⁶ Upper limits in Table 5 are not considered when deriving differences between Mg I and Mg II-based abundances.

Table 5. Average LTE and N-LTE magnesium abundances in the program stars from Mg I and Mg II lines.

Star	[MgI/H] _{LTE}	[MgI/H] _{N-LTE}	[MgII/H] _{LTE}	[MgII/H] _{N-LTE} ^a	Δ [Mg/H] _{LTE}	Δ [Mg/H] _{N-LTE}
HD 400	-0.09	-0.04	-0.09	-0.15	+0.00	-0.11
HD 4614	-0.40	-0.35	-0.42	-0.43	-0.02	-0.08
HD 19994	+0.17	+0.24	+0.06	+0.00	-0.11	-0.24
HD 51530	-0.32	-0.25	-0.39	-0.44	-0.07	-0.19
HD 59984	-0.49	-0.43	-0.41	-0.43	+0.08	+0.00
HD 106516	-0.52	-0.47	-0.57	-0.60	-0.05	-0.13
HD 116316	-0.59	-0.50	-0.59	-0.62	+0.00	-0.12
HD 134169	-0.56	-0.49	-0.35	-0.39	+0.19	+0.10
HD 150177	-0.74	-0.65	< -0.60	< -0.64	< +0.14	< +0.01
HD 165908	-0.63	-0.57	-0.60	-0.62	+0.03	-0.05
HD 170153	-0.52	-0.43	-0.50	-0.53	+0.02	-0.10
HD 192718	-0.44	-0.38	< -0.40	< -0.42	< +0.04	< -0.04
HD 201891	-0.82	-0.79	< -0.65	< -0.65	< +0.17	< +0.14
HD 207978	-0.59	-0.49	-0.45	-0.50	+0.14	-0.01
HD 208906	-0.73	-0.64	< -0.50	< -0.51	< +0.23	< +0.13
HD 210595	-0.52	-0.47	-0.52	-0.60	+0.00	-0.13
HD 210752	-0.59	-0.57	-0.47	-0.49	+0.12	+0.08
HD 215257	-0.66	-0.59	< -0.60	< -0.61	< +0.06	< -0.02
BD +18° 3423	-0.94	-0.91	-0.97	-0.98	-0.03	-0.07
Average					+0.021	-0.077
Dispersion					± 0.081	± 0.091

^a Note that the abundances shown are those obtained after considering the N-LTE corrections in the Sun.

with those of thin disk stars of similar metallicity (e.g. HD 170153 and HD 210752) supports with this statement. Thus, at least in part, the scatter in the [Mg/Fe] ratios that we found in the range $-0.7 \lesssim [\text{Fe}/\text{H}] \lesssim -0.5$ may be due to this fact (see Figure 5).

4.2 Magnesium and oxygen

To finish this section we shall use the results described above to address the issue of the oxygen problem in metal-poor stars in an indirect way. We found a good agreement between the Mg abundances derived from neutral lines of different excitation energies and those derived from Mg II lines, which have a similar excitation energy to that of the O I triplet. When N-LTE corrections are applied to Mg abundances, the agreement between the different Mg indicators remains. In consequence, the [Mg/Fe] vs. [Fe/H] relationship obtained from the Mg I and Mg II lines is essentially the same and agrees with the widely accepted behaviour of α -elements in metal-poor stars. This would indicate that when the classical 1D analysis is used, these Mg II lines can be considered as *good indicators* of the Mg abundance in metal-poor stars, at least in the metallicity range studied here. Let us now consider the consequences of this result with respect to the oxygen triplet-based abundances.

During the last decade, several approaches have been used to solve the oxygen problem (see an update of the present status in e.g., Nissen et al. 2002 or Fullbright & Johnson 2003). First, it is well known that the formation of the O I triplet in late-type stars is affected by departures from LTE. The higher the temperature and the lower the gravity of the star, the greater is this effect. However, detailed N-LTE computations (e.g. Eriksson & Toft 1979;

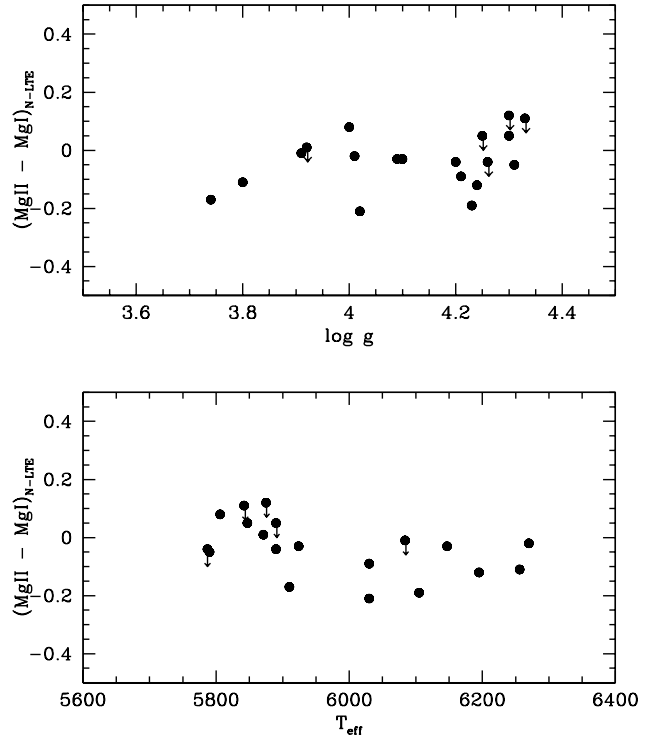


Figure 4. Difference between the N-LTE magnesium abundances from Mg I and Mg II lines against the effective temperature and gravity of the stars. No correlation is seen.

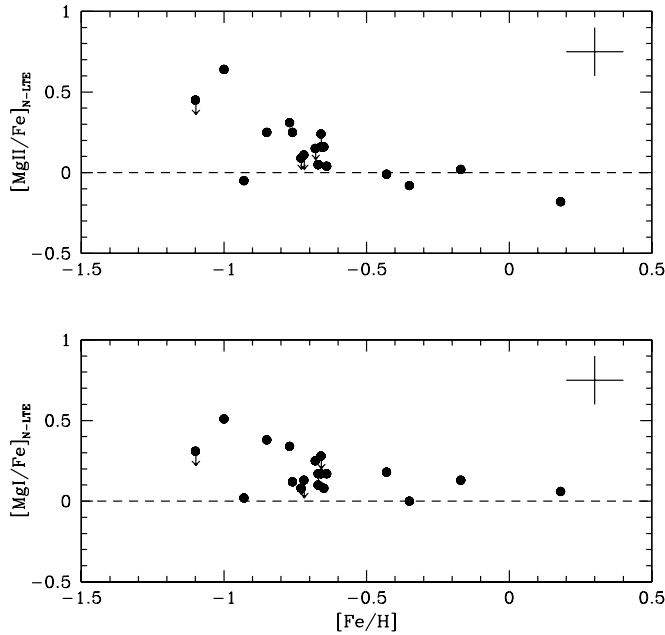


Figure 5. $[\text{Mg}/\text{Fe}]$ vs. $[\text{Fe}/\text{H}]$ relationship in the sample stars from Mg I and Mg II N-LTE abundances.

Takeda 1992, 1994, 2003; Kiselman 2001) have repeatedly shown that N-LTE corrections are not enough make the oxygen abundances derived from the triplet agree with those obtained from the [OI] features⁷.

On the other hand, it has also been argued that because of their *high excitation energy* ($\chi = 9.14$ eV) the oxygen triplet forms deep in the photosphere where *inhomogeneities due to granulation* are expected to be large (obviously, granulation cannot be considered in the standard 1D model atmosphere). In Table 6, we compare the average formation depth of the Mg II lines with that of the two weakest lines of the oxygen triplet (those with a similar strength to that of the Mg II lines) in three stars of our sample that cover the range of stellar parameters studied here. As an illustration, the last line in Table 6 shows the case of a star with stellar parameters $T_{\text{eff}} = 6000$ K, $\log g = 4.0$ and $[\text{Fe}/\text{H}] = -2$. [The oxygen problem is mainly found in stars with $[\text{Fe}/\text{H}] \lesssim -1.5$ where, unfortunately, it is very difficult to detect the Mg II lines]. The calculations were made assuming an oxygen enhancement of $[\text{O}/\text{Fe}] \sim +0.5$, which is typical for a star with $[\text{Fe}/\text{H}] \sim -1$. Although the concept of formation depth is quite ambiguous, since a single line may sample very different layers of the atmosphere (Ruiz-Cobo & del Toro Iniesta 1994; Sánchez Almeida et al. 1996), in the case of weak spectral lines it might still be used for a qualitative discussion. On this basis, Table 6 shows that the O I triplet and the Mg II lines do not differ significantly in the depth of formation. The oxygen lines form in slightly higher layers; nonetheless,

Table 6. Averaged formation depths over the line profile for the Mg II lines and O I triplet.

Star/Model	$\log \tau_{5000}$			
	MgII 7877	MgII 7896	OI 7774	OI 7775
HD 51530	-0.20	-0.20	-0.44	-0.38
HD 59984	-0.18	-0.20	-0.40	-0.32
BD +18° 3423	-0.08	-0.12	-0.22	-0.17
6000/4.0/-2.0	+0.00	-0.05	-0.14	-0.14

from the point of view of 1D model atmosphere structure and modelling, this difference is not important. Therefore, from the point of view of 1D analysis, any systematic effect introduced by an incorrect temperature scale, by inhomogeneities etc, should affect the Mg II lines and the O I triplet in a similar way. Since no systematic differences were found between Mg I and Mg II abundances, we might say that the oxygen abundances derived from the triplet should also be free of these atmospheric problems. In other words, O I triplet-based abundances in metal-poor stars may be wrong, but our results concerning Mg II abundances argue against this reasoning. This conclusion must be confirmed by deriving magnesium abundances from the Mg II lines in a large sample of very metal-poor stars ($[\text{Fe}/\text{H}] \lesssim -1.5$), where the oxygen problem really exists. Of course, in 3D model atmosphere analyses the concept of the formation depth of a given line is meaningless since in some parts of the atmosphere (e.g. warm up-flows) the line is formed at a given depth while in other parts (e.g. cool down-flows) the line may be formed at quite a different depth. However, for lines having very similar excitation energies and belonging to majority species (as do the Mg II and O I triplet lines), large differences in the 3D effects are not expected (M. Asplund, private communication). Thus, the conclusion above in 1D may hold when 3D atmospheres are used. Studies of 3D N-LTE formation of O I and Mg II lines in metal-poor stars are urgently needed to confirm this.

As an additional test, we compared the $[\text{O}/\text{Mg}]$ vs. $[\text{Fe}/\text{H}]$ ratios derived using Mg I and Mg II lines. This is shown in Figure 6. From the literature, we took the equivalent width measurements of the O I triplet in stars in common with this work and derived oxygen abundances according to the stellar parameters shown in Table 2. The spectroscopic data for the O I triplet were taken from Kurucz & Bell (1995). The standard van der Waals damping constant from Unsöld was modified to fit the equivalent widths of the O I triplet in the solar flux spectrum (Kurucz et al. 1984), adopting a solar oxygen abundance of $\log \epsilon(\text{O}) = 8.69$ (Allende Prieto et al. 2001). Oxygen abundances were corrected from N-LTE effects according to the formula given by Takeda (2003) (see his equation 1) which takes into account the dependence of this correction on T_{eff} and $\log g$ ⁸. Therefore, Figure 6 shows N-LTE $[\text{O}/\text{Mg}]$ ratios.

It can be seen that the of the $[\text{O}/\text{Mg}]$ ratios from Mg I and Mg II abundances are positive. $[\text{O}/\text{Mg}]$ from Mg II lines are a little higher on average due to the sign of the N-

⁷ By the way, we should comment that, although with a less complete O I atom model, N-LTE effects on the triplet were considered by Sneden et al. (1979) and Abia & Rebolo (1989). These authors reached the same conclusions as the most recent and detailed N-LTE studies.

⁸ Takeda (2003) does not find any dependence of N-LTE corrections on the O I triplet with the metallicity.

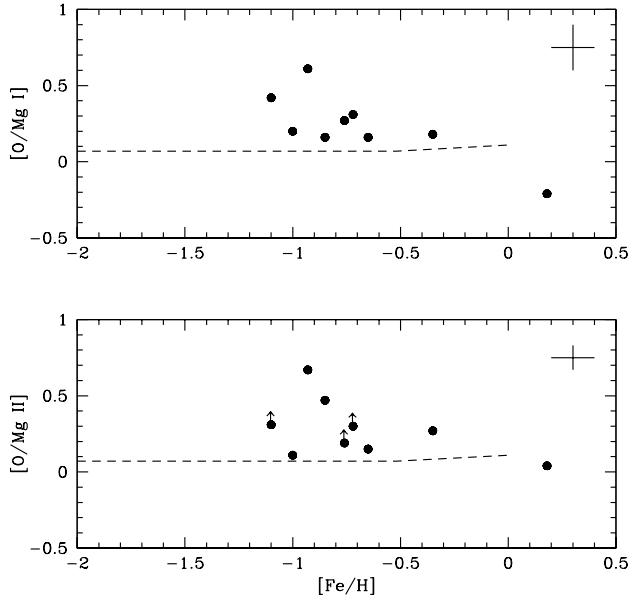


Figure 6. $[O/Mg]$ vs. $[Fe/H]$ relationship in the sample stars obtained from N-LTE Mg I and Mg II abundances. The dashed line connects the predicted $[O/Mg]$ ratio according to the yields obtained by Limongi & Chieffi (2002) from type II supernova models and their dependence on the metallicity of the progenitor (see text). Note the different error bar in $[O/Mg]$. This is because uncertainties in the atmosphere parameters affect the Mg I and Mg II lines in opposite senses.

LTE corrections (see Sect. 3). The point at $[O/Mg] \sim +0.7$ is the star BD +18° 3423 which has an unusually low Mg abundance (see Table 5) considering that it is a halo star. Mashonkina et al. (2003) also derive a low Mg abundance ($[Mg/Fe] = +0.12$) for this star as well as for other halo stars, suggesting that the halo stellar population may be inhomogeneous by origin. In any case, despite the low number of stars and considering the errors in the $[O/Mg]$ ratios (see Figure 6), we can say that the $[O/Mg]$ ratio is constant in the metallicity range of our stars. Carretta et al. (2000), using both [OI] and O I lines (but only Mg I lines), find $[O/Mg]$ ratios at the same level of enhancement and with similar scatter at a given metallicity in stars with $-2.5 \lesssim [Fe/H] \lesssim -1$.

In Figure 6, the dashed line represents the predicted $[O/Mg]$ ratio according to the SNII explosion models by Limongi & Chieffi (2002). These SNII models cover the mass $13 \lesssim M/M_{\odot} \lesssim 40$ and metallicity $Z = 0.02$ to 10^{-6} ranges. The line was computed by integrating the yields in the mass and metallicity ranges with Salpeter’s standard IMF. Clearly, most of the observed $[O/Mg]$ values are well above this line, even considering the error bars⁹. There are at least two possible explanations of this discrepancy between theory and observations:

i) Since most of the $[O/Mg]$ ratios in the literature (including the present work) are derived from the O I triplet, this would indeed indicate that the oxygen abundances de-

rived from these lines are too large, for as yet unknown reasons (see Fullbright & Johnson 2003, for a discussion of several alternative explanations). However, note that in the metallicity range studied here, all the oxygen indicators agree using 1D and/or 3D atmosphere models (see Nissen et al. 2002). Thus, eventually $[O/Mg]$ ratios derived from oxygen indicators other than the oxygen triplet would give similar ratios (at least in stars with $-1.0 \lesssim [Fe/H] \lesssim 0.0$). However, very recently Bensby et al. (2003) studied the $[O/Mg]$ vs. $[Fe/H]$ relationship in a sample of stars with metallicity from $[Fe/H] \approx -0.9$ to $+0.4$ using oxygen abundances from the [OI] 6300 Å line. Their $[O/Mg]$ are in closer agreement with the theoretical expectations, suggesting indeed that the OI triplet lines are not good abundance indicators. They noted also that oxygen does not follow magnesium at super-solar metallicities as the $[O/Mg]$ ratio in the star with $[Fe/H] > 0.0$ in Figure 6 may suggest.

ii) Oxygen and/or magnesium yields in SNII models are wrong. However, oxygen and magnesium are produced mainly during hydrostatic burning in the SNII progenitor and only a small fraction of the ejecta stems from explosive neon- and carbon-burning (e.g. Thielemann et al. 1996). Therefore, their yields should not be greatly affected by uncertainties in the SNII explosion model. Instead, the actual value of the $^{12}C(\alpha, \gamma)^{16}O$ reaction rate and the treatment of rotation and convection during the hydrostatic phases may affect the O and Mg yields. This uncertainty, however, would be translated into a variation of no more than ± 0.1 dex in the position of the dashed line in Figure 6 (see the discussions by Argast et al. 2002; Heger & Langer 2000; Imbriani et al. 2001), and the discrepancy between theory and observations would remain.

iii) Finally, we should take into account that the formation of spectral lines in metal-poor atmospheres is not fully understood yet and, therefore, any conclusion extracted from the $[X/Fe]$ vs. $[Fe/H]$ studies on the chemical evolution of the Galaxy should be considered with caution. Let us remember the recent discrepancy found between the observed and the predicted primordial Li abundances from Big-Bang nucleosynthesis as inferred by the WMAP analysis of the cosmic microwave background (Bennett et al. 2003). Obviously, homogeneous and 3D studies of the $[O/Mg]$ ratio in a larger sample of stars are needed to answer this question.

5 SUMMARY

We have analysed several Mg I and two Mg II lines in a sample of 19 mildly metal-poor dwarf stars in a search for differences between these two Mg abundance indicators. We found a good agreement between both in the LTE and N-LTE cases. Similar to the features found in other studies, the $[Mg/Fe]$ ratios derived here show significant scatter at $[Fe/H] \sim -0.6$ which is currently ascribed to the existence of thick and thin disk stars at about this metallicity, stars which are chemically discrete from each other. Using the oxygen abundances from the literature, we also studied the $[O/Mg]$ vs. $[Fe/H]$ relationship. The $[O/Mg]$ ratios derived are constant over the range of metallicity studied but significantly larger than the nucleosynthetic predictions obtained from SNII models. There is no easy explanation to this problem. It could be both spectroscopic and theoretical but, in

⁹ Note that using a higher oxygen abundance in the Sun (e.g. 8.87, Grevesse & Sauval 1998) to derive the $[O/Mg]$ ratio, the resulting line would be ~ 0.1 dex below.

any case, the determination of any abundance ratio in metal-poor stars urgently requires a detailed modelling (3D) of their atmospheres as well as a simultaneous N-LTE study. Only thus could we safely draw conclusions concerning the chemical evolution of the Galaxy.

ACKNOWLEDGEMENTS

Data from the VALD database at Vienna were used for the preparation of this paper. The 2.5m NOT telescope is operated on the island of La Palma by the RGO in the Spanish Observatory of the Roque de los Muchachos of the Instituto de Astrofísica de Canarias. This work was also based in part on observations collected with the 2.2m telescope at the German-Spanish Astronomical Centre, Calar Alto (Almería). It was partially supported by the Spanish grant AYA2002-04094-C03-03 from the Ministerio de Ciencia y Tecnología. ML thanks RBRF (grant 02-02-17174) and the RF President on Leading Scientific Schools (grant 1789.2003.2) for partial financial support. We thank the referee for the valuable comments and criticism which served to improve this work considerably.

REFERENCES

- Abia C., Rebolo R., 1989, *ApJ*, 347, 186
- Allen C.W., 1973, *Astrophysical Quantities*, Athlone Press (London)
- Allende Prieto C., Lambert D.L., Asplund M., 2001, 556, L63
- Alonso A., Arribas S., Martínez-Roger C., 1996, *A&AS*, 117, 227
- Alonso A., Arribas S., Martínez-Roger C., 1995, *A&A*, 297, 197
- Alonso A., Arribas S., Martínez-Roger C., 1994, *A&AS*, 107, 365
- Aoki W., Norris J.E., Ryan S.G., Beers T.C., Ando H., 2002, *PASJ*, 54, 933
- Argast D., Samland M., Thielemann F.-K., Gerhard O.E., 2002, *A&A*, 388, 842
- Asplund M., 2003, in *CNO in the Universe*, C. Charbonnel, D. Schaerer, G. Meynet. ASP Conference Series, p. 275
- Asplund M., Nordlund Å., Trampedach R., Stein R.F., 1999, *A&A*, 346, L17
- Asplund M., García-Pérez A.E., 2001, *A&A*, 372, 601
- Asplund M., Nordlund Å., Trampedach R., Allende-Prieto C., Stein R.F., 2000, *A&A*, 359, 743
- Athay R.G., Canfield R.C., 1969, *ApJ*, 156, 695
- Auer L.H., Heasley J.N., 1976, *ApJ*, 205, 165
- Barklem P.S., Belyaev A.K., Asplund M., 2003, *A&A*, 409, L1
- Barbuy B., Spite F., Spite M., 1985, *A&ASS*, 144, 343
- Bellot-Rubio L.R., Borrero J.M., 2002, *A&A*, 391, 331
- Bennett C.L., Halpern M., Hinshaw G., et al., 2003, *ApJS*, 148, 1B
- Bensby T., Feltzing S., Lundström I., 2003, *A&A*, 410, 527
- Barnes K.R., 1971, *Monograph on applied Optics*, Bristol: A. Hilger of the Pacific, p. 410
- Biémont E., Baudoux M., Kurucz R.L., Ansbacher W., Pinnington E.H., 1991, *A&A*, 249, 539
- Butler K., Mendoza C., Zeppen C.J., 1984, *MNRAS*, 209, 343
- Carney B.W., 1983, *AJ*, 88, 610
- Carretta E., Gratton R.G., Sneden C., 2000, *A&A*, 356, 238
- Cayrel R., 1988, in *The Impact of Very High S/N Spectroscopy on Stellar Physics*, ed. G. Cayrel de Strobel and M. Spite (Dordrecht: Kluwer), p.345
- Chen Y.Q., Nissen P.E., Zhao G., Zhang H.W., Benoni T., 2000, *A&AS*, 141, 491
- Cunto W., Mendoza C., Ochsenbein F., Zeppen C.J., 1993, *A&A*, 257, L5
- Depagne E., Hill V., Christlieb N., Primas F., 2000, *A&A*, 346, L6
- Drawin H.W., 1968, *Z. Phys.*, 211, 404
- Edvardsson B., Andersen J., Gustafsson B., Lambert D.L., Nissen P.E., Tomkin J., 1993, *A&A*, 275, 101
- Eriksson K., Toft S.C., 1979, *A&A*, 71, 178
- ESA 1997, *The Hipparcos and Tycho Catalogues* (ESA SP-1200) (Noordwijk: ESA)
- Finlator K., Ivezić Z., Fan X., et al., 2000, *AJ*, 120, 2615
- Fuhrmann K., 2004, *Astron. Nachrichten* (in press)
- Fuhrmann K., 1998, *A&A*, 338, 161
- Fuhrmann K., Axer M., Gehren T., 1995, *A&A*, 301, 492
- Fulbright P., Johnson J.A., 2003, *ApJ*, 595, 1181
- Gehren T., Liang Y.C., Shi J.R., Zhang H.W., Zhao G., 2004, *A&A*, 413, 1045
- Gratton R.G., Carretta E., Desidera S., Lucatello S., Mazzei P., Barbieri M., 2003a, *A&A*, 406, 131
- Gratton R.G., Carretta E., Claudi R., Lucatello S., Barbieri M., 2003b, *A&A*, 404, 187
- Gratton R.G., Carretta E., Eriksson K., Gustafsson B., 1999, *A&A*, 350, 955
- Gratton R.G., Carretta E., Castelli F., 1996, *A&A*, 314, 191
- Grevesse N., Sauval A.J., 1998, *Space Sci. Rev.*, 85, 161
- Heger A., Langer N., 2000, *ApJ*, 544, 1016
- Hibbert A., Dufton P.L., Murray M.J., York D.G., 1983, *MNRAS*, 205, 535
- Hofsaess D., 1979, *ADNDT*, 24, 285
- Holweger H., Müller E.A., 1974, *Solar Physics*, 39, 19
- Idiart T., Thévenin, F., 2000, *ApJ*, 541, 207
- Imbriani G., Limongi M., Gialanella L., et al., 2001, *ApJ*, 558, 903
- Kiselman D., 2001, *New Astronomy Rev.*, 45, 559
- Korn A.J., Shi, J., Gehren T., 2003, *A&A*, 407, 691
- Kupka F., Piskunov N., Ryabchikova T.A., Stempels H.C., Weiss W.W., 1999, *A&AS*, 138, 119
- Kurucz R.L., 1998, [HTTP://cfaku5.harvard.edu](http://cfaku5.harvard.edu)
- Kurucz R.L., Bell B., 1995, CD-ROM No. 23 (Harvard-Smithsonian Center for Astrophysics)
- Kurucz R.L., Furenlid I., Brault J., Testerman L., 1984, *Solar Flux Atlas from 296 to 1300 nm*, National Solar Observatory, Sunspot, New Mexico
- Kurucz R.L., Peytremann E., 1975, *SAO Special Report* 362, part 1
- Kwong H.S., Smith P.L., Parkinson W.H., 1982, *Physical Review A*, 25, 2629
- Lambert D.L., Luck R.E., 1978, *MNRAS*, 183, 79
- Limongi M., Chieffi A., 2002, *PASP*, 19, 246
- Magain P., 1989, *A&A*, 209, 211
- Mashonkina L., Gehren T., Travaglio C., Borkova T., 2003, *A&A*, 397, 275
- Mashonkina L., Gehren T., 2001, *A&A*, 376, 232
- Mashonkina L., Gehren T., Bikmaev I.F., 1999, *A&A*, 343, 519
- Mashonkina L., Shimanskaya N.N., Sakhibullin N.A., 1996, *Astronomy Reports*, 40, 212
- Mauas P.J., Avrett E.H., Loeser R., 1988, *ApJ*, 330, 1008
- Mihalas D., 1978, *Stellar Atmospheres*, 2nd ed. (San Francisco: W.H. Freeman and Company)
- Mihalas D., 1972, *ApJ*, 177, 115
- Nissen P., Primas F., Asplund M., Lambert D.L., 2002, *A&A*, 390, 235
- Nissen P.E., Schuster W.J., 1997, *A&A*, 326, 751
- Norris J.E., Ryan S.G., Beers T.C., 2001, *ApJ*, 561, 1034
- Nordlund Å., Dravins D., 1990, *A&A*, 228, 203
- Oertel G.K., Shomo L.P., 1968, *ApJS*, 16, 175
- Pfeiffer M.J., Frank C., Baumüller D., Fuhrmann K., Gehren T., 1998, *A&A*, 130, 381

- Prochaska J.X., Naumov S.O., Carney B.W., McWilliam A., Wolfe A., 2000, *AJ*, 120, 2513
- Przybilla N., Butler K., Becker S.R., Kudritzki R.P., 2001, *A&A* 369, 1009
- Qiu H.M., Zhao G., Takada-Hidai M., Chen Y.Q., Takeda Y., Noguchi K., Sadakane K., Aoki W., 2002, *PASJ*, 54, 103
- Reddy B.E., Tomkin J., Lambert D.L., Allende Prieto C., 2003, *MNRAS*, 340, 304
- Ruiz-Cobo B., del Toro Iniesta J.C., 1994, *A&A*, 283, 129
- Sakhibullin N.A., 1983, *TrKaz*, 48, 9
- Samland M., Gerhard O.E., 2003, *A&A*, 399, 961
- Sánchez-Almeida J., Ruiz-Cobo B., del Toro Iniesta J.C., 1996, *A&A*, 314, 295
- Snedden C., Lambert D.L., Whitaker R.W., 1979, *ApJ*, 234, 964
- Steenbock W., Holweger H., 1984, *A&A*, 130, 319
- Schuster W.J., Nissen P.E., 1988, *A&AS*, 73, 225
- Schuster W.J., Nissen P.E., 1989, *A&A*, 221, 65
- Sigut T.A.A., Lester J.B., 1996, *ApJ*, 461, 972
- Sigut T.A.A., Pradhan A.K., 1996, *A&AS*, 189, 9807
- Snijders M.A.J., Lamers H.J.G.L.M., 1975, *A&A*, 41, 245
- Takeda Y., 1992, *PASJ*, 44, 309
- Takeda Y., 1994, *PASJ*, 46, 53
- Takeda Y., 2003, *A&A*, 402, 343
- Taylor B.J., 2003, *A&A*, 398, 731
- Thévenin F., Idiart T., 1999, *ApJ*, 521, 753
- Thévenin F., 1990, *A&ASS*, 82, 179
- Thielemann F.-K., Nomoto K., Hashimoto M., 1996, *ApJ*, 460, 408
- Truran J.W., Cowan J.J., Pilachowski C.A., Sneden C., 2002, *PASP*, 114, 1293
- Tuominen I., Ilyin I., Petrov P., 1998, in *Astrophysics with the NOT*, H. Karttunen and V. Pirola Eds., p. 147
- Unsöld A., 1955, *Physik der Sternatmosphären* (Springer Verlag, Berlin)
- VandenBerg D.A., Bell R.A., 2001, *New astronomy Rew.*, 45, 577
- VandenBerg D.A., Sweson F.J., Rogers F.J., Iglesias C., Alexander D.R., 2000, *ApJ*, 532, 430
- van Regemorter H., 1962, *ApJ*, 136, 906
- Weimberg D.H., Hernquist L., Katz N., 2002, *ApJ*, 571, 15
- Wiese W.L., Fuhr J.R., Deters T.M., 1969, *J. Phys. Chem. Ref. Data*, Monograph No. 7
- Zhao G., Gehren T., 2000, *A&A*, 362, 1077
- Zhao G., Butler K., Gehren T., 1998, *A&A*, 333, 219